Progress In Electromagnetics Research M, Vol. 26, 69–84, 2012

COMPUTATION OF THE MODES OF ELLIPTIC WAVEGUIDES WITH A CURVILINEAR 2D FREQUENCY-DOMAIN FINITE-DIFFERENCE APPROACH

A. Fanti*, G. Mazzarella, G. Montisci, and G. A. Casula

Dipartimento di Ingegneria Elettrica ed Elettronica, Università di Cagliari, Piazza d'Armi, Cagliari 09123, Italy

Abstract—A scalar Frequency-Domain Finite-Difference approach to the mode computation of elliptic waveguides is presented. The use of an elliptic cylindrical grid allows us to take exactly into account the curved boundary of the structure and a single mesh has been used both for TE and TM modes. As a consequence, a high accuracy is obtained with a reduced computational burden, since the resulting matrix is highly sparse.

1. INTRODUCTION

Elliptic waveguides have been used as guiding structures, and in different applications as components in waveguide circuits. Among the latter, we can quote their use as matching sections between circular and rectangular waveguides [1], or for the realization of low sensitivity irises in dual mode filters [2].

In many applications, the knowledge of both eigenvalues and field distributions of waveguides modes is required. Among them, there are the analysis of waveguide junctions using mode matching [3, 4] and the solution of waveguide problems with sources [5]. The same type of information is also required in the analysis, using the method of moments (MoM), of thick-walled apertures [6–10] and waveguide junctions [11, 12]. Indeed, these apertures can be considered as stub waveguides, and the modes of these guides are the natural basis functions for MoM.

Analytic computation of the modes is simple and accurate only for rectangular and circular waveguides, since the mode distribution can be expressed [5] in terms of trigonometric or Bessel Functions,

Received 8 August 2012, Accepted 18 September 2012, Scheduled 25 September 2012

* Corresponding author: Alessandro Fanti (alessandro.fanti@diee.unica.it).

and the eigenvalues are the zeroes of these functions. An analytical, closed form solution exists also for elliptic waveguides, and has been found by Chu [13] since the 30's. Unfortunately, the field distribution is described by the Mathieu functions [14], whose numerical evaluation is very cumbersome. The best approach seems the expansion of those functions in a series of (more tractable) Bessel functions [15]. As a consequence, the eigenvalues of an elliptic guide must be computed numerically, looking for the zeroes of a suitable series of Bessel functions. Then, the field distribution of each mode requires further evaluations of Mathieu functions. It is not a surprise, therefore, that the availability of a closed-form solution in this case have not prevented many different approximate [16] or numerical techniques [17] to be proposed. All of them, however, require a trade off between simplicity and reduced computational load from one side, and accuracy from the other. This is true also for standard use of general purpose numerical techniques, such as Finite Differences and Finite Elements. In particular, the Frequency-Domain Finite-Difference approach (FDFD) [18], namely the direct discretization of the differential eigenvalue problem, is the simplest strategy. FDFD method can be applied both to scalar and vector problems. In particular for metallic waveguides, the formulation in terms of scalar potentials allows a significant reduction of the computational load. As a matter of fact, the vector FDFD approach leads to a constrained eigenvalue problem [19], which is computationally heavy since it requires the computation of the eigenvectors of a full matrix, instead of a sparse matrix as in the case of the scalar approach.

The standard FDFD approach, using a cartesian sampling grid, allows a very effective solution for rectangular waveguides or generic rectangular guiding structures, since in these cases the boundary is perfectly fitted to the discretization grid, either uniform [20] or non-uniform [21]. On the other hand, the standard FDFD requires, for generic curved structures, a staircase approximation of the boundary [22–24]. As a consequence, its effectiveness (computational burden vs accuracy) is lowered and, for example in the case of elliptic guides, it becomes comparable to Chu solution, even using sparse matrix techniques for eigenvalues evaluation.

In the open literature, a number of papers are available dealing with the use of curvilinear grids in finite difference methods, both for vector FDFD [25] and for FDTD applications [26]. However, FDTD method is cumbersome and computationally heavy when the solution of either 2D [27] or 3D [28] eigenvalue problems is required.

An important drawback of the scalar FDFD approach is the requirement of two different grids for TE and TM modes, justified

with the different boundary conditions. This means that TE and TM modes are not known in the same sampling points. On the other hand, in mode matching and other applications, TE and TM modes need to be considered together, and in the same points, which prevents the results of a standard scalar FDFD method to be easily used. This approach has been proposed in [29] for rectangular waveguides, but its use is even more significant for elliptic guides, since (at variance of rectangular waveguides) no simple transformations between standard TE and TM grid are then available.

Aim of this work is to further improve the FDFD approach for elliptic waveguide sections to reach the effectiveness of the rectangular case. The main step is the use of an elliptic cylindrical coordinate system, both for the eigenvalue equations and for the grid points of the FD. In this way the FDFD method is able to take exactly into account the curved boundary of the waveguide and therefore with no loss of accuracy. We consider first the use of two different grids for TE and TM modes, each one tailored to the BC of those modes. Then we will show how to use a single grid to compute, with the same computational costs, both TE and TM modes, so that all modes are sampled on the same set of points.

The presented technique allows a significant improvement of the accuracy of the standard FDFD at equal discretization step, and a better flexibility.

2. DESCRIPTION OF THE TECHNIQUE

2.1. Fundamentals of the Scalar FDFD Approach

Let us consider a generic waveguide. Both TE and TM modes can be found [5] from a suitable scalar eigenfunction of the Laplace operator:

$$\nabla_t^2 \phi + k_t^2 \phi = 0 \tag{1}$$

with the boundary conditions (BC)

$$\begin{aligned} \frac{\partial \phi}{\partial n} &= 0 \qquad \text{TE} \\ \phi &= 0 \qquad \text{TM} \end{aligned} \tag{2}$$

wherein the subscript t in (1) indicates that the Laplace operator is computed with respect to the transverse coordinates and ϕ is a scalar function of the transverse coordinates. In (2) the derivative is with respect to the unit normal to the transverse waveguide boundary, $\underline{i}_n$, pointing outward.

FDFD approach prescribes to replace both the Equation (1) and the BC (2) by a discretized version, looking for the eigenfunction values at a suitable set of sampling points, and therefore replacing derivatives with finite approximations. The discretized version of (1) consists of one equation for each discretization point, which depends, for boundary points, also on the BC (2). Therefore (1, 2) is replaced by an equivalent matrix algebraic eigenvalue problem. The resulting matrix is sparse so a very effective computation is possible.

If the waveguide boundary consists of straight lines, parallel to the coordinate axes, the problem can be discretized on a cartesian grid [30]. This grid defines also a partition of the waveguide surface into rectangular cells, which fill exactly the waveguide section. For every other waveguide, the section cannot be exactly partitioned using rectangular cells and this leads to numerical errors unless a very fine mesh is used.

The alternative, to get a high accuracy, is to use a different discretization scheme, which matches exactly the waveguide boundary. Therefore, the discretization nodes must be at the intersections of a suitable framework, in which the waveguide boundary is a coordinate curve. In this way the waveguide section is exactly partitioned into discretization cells. The discretized equations can then be obtained in two ways. Either we use a Taylor expansion of ϕ between each pair of discretization points as in standard (rectangular) FD approach [17], or we can integrate (1) over a discretization cell S_F, with boundary Γ_F:

$$\int_{S_F} \nabla_t^2 \phi \; dS = -k_t^2 \int_{S_F} \phi \; dS \tag{3}$$

Use of Gauss Theorem gives:

$$\int_{\Gamma_F} \nabla_t \phi \cdot \mathbf{i}_n \; dl = \int_{\Gamma_F} \frac{\partial \phi}{\partial n} \; dl = - \; k_t^2 \int_{S_F} \phi \; dS \; = -k_t^2 \phi_X \; \hat{S} \tag{4}$$

where $\mathbf{i}_n$ is the normal to Γ_F, pointing outward, ϕ_X the value at the discretization point of cell S_F, and $\hat{S}$ the cell area. So Equation (4) becomes:

$$\frac{1}{\hat{S}} \int_{\Gamma_F} \frac{\partial \phi}{\partial n} \; dl = -k_t^2 \phi_X \tag{5}$$

To evaluate the left hand side, Γ_F is divided into (curved) segments, along the coordinate curves, and the normal derivative is evaluated in finite terms.

The two approaches apply in overlapping cases, and, when both can be used, the resulting discretized equation is the same. Since both discretizations (either the standard finite approximation and that

based on (5)) can take into account the BC (2), the resulting FD formulation is equivalent to the complete eigenvalue problem (1,2).

2.2. Elliptic Waveguide

Let us consider an elliptic waveguide. We build up the discretization grid using the coordinate lines of the elliptic cylindrical framework (u, v) (Figure 1). Assuming a regular spacing on the coordinate lines, with step $\Delta u, \Delta v$, the standard sets of grid points for TE and TM modes are shown in Figure 2.

Letting $\phi_{ij} = \phi(i\Delta u, j\Delta v)$, the eigenvalue Equation (1) can be expressed as:

$$\frac{1}{h(i\Delta u, j\Delta v)^2} \cdot \left[\frac{\partial^2 \phi}{\partial u^2} + \frac{\partial^2 \phi}{\partial v^2}\right]_{ij} = -k_t^2 \phi_{ij} \tag{6}$$

wherein $h(u, v) = a\sqrt{\sinh^2 u + \sin^2 v}$ is the scale factor of the elliptic cylindrical coordinate system and $2a$ the distance between the foci (see Figure 1).

For internal points, such as P of Figure 3, it is simpler to discretize (6) using a Taylor expansion, since the term in brackets is expanded exactly as in a rectangular grid [30]:

$$\left[\frac{\partial^2 \phi}{\partial u^2} + \frac{\partial^2 \phi}{\partial v^2}\right]_P = \frac{\phi_A}{\Delta v^2} + \frac{\phi_B}{\Delta u^2} + \frac{\phi_C}{\Delta v^2} + \frac{\phi_D}{\Delta u^2} - \left(\frac{2}{\Delta u^2} + \frac{2}{\Delta v^2}\right) \cdot \phi_P \tag{7}$$

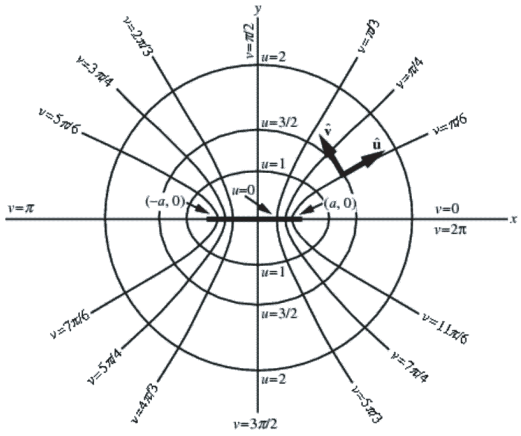

Figure 1. Geometry of the elliptic cylindrical coordinates.

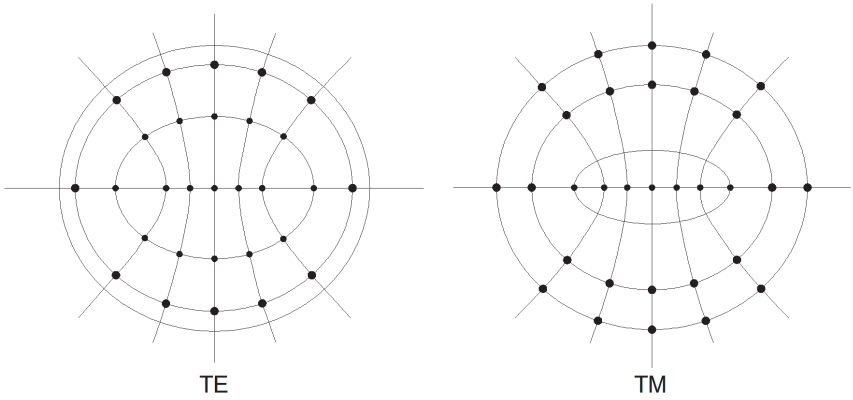

Figure 2. Standard TE and TM elliptic grids, as suggested from BC.

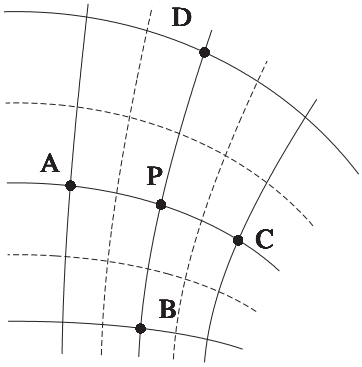

Figure 3. Internal point of TE or TM grid.

Then, using (6) and (7), we get the discretized form of (1) for a generic point (i, j):

$$-h_{ij}^2 k_t^2 \phi_{ij} = \frac{\phi_{i,j-1}}{\Delta v^2} + \frac{\phi_{i-1,j}}{\Delta u^2} + \frac{\phi_{i,j+1}}{\Delta v^2} + \frac{\phi_{i+1,j}}{\Delta u^2} - \left(\frac{2}{\Delta u^2} + \frac{2}{\Delta v^2} \right) \cdot \phi_{i,j} \quad (8)$$

wherein $h_{ij} = h\,(i\Delta u, j\Delta v)$.

Equation (8) is valid for all internal points, except the singularities of the ellipse, namely the foci and the points between them. Also boundary points must be considered apart. In the following subsections we will address these particular cases.

2.2.1. Boundary Points

The discretized Equation (7) must be modified for a boundary point, in order to include the BC (2). Since the BC are different for TE and TM modes, the standard solution, widely used for the rectangular grid case, is to use two different grids, one for TE and the other for TM modes, as in Figure 2.

In the TM case, the standard approach requires that each boundary point D is a sampling point, so that $\phi_D = 0$ (see Figure 2(b)), which can be directly put into the discrete Equation (7), written for point P, to get:

$$\left[\frac{\partial^2\phi}{\partial u^2} + \frac{\partial^2\phi}{\partial v^2}\right]_P = \frac{\phi_A}{\Delta v^2} + \frac{\phi_C}{\Delta v^2} + \frac{\phi_B}{\Delta u^2} - \left(\frac{2}{\Delta u^2} + \frac{2}{\Delta v^2}\right)\cdot\phi_P \qquad (9)$$

On the other hand, for the TE case, no discretization points are on the boundary, as clear from Figure 4(a), since X is not a discretization point (compare Figure 2). Use of Taylor expansion would therefore require an extrapolation of $\phi(u)$ outside the sampling region, using either ϕ_X or ϕ_Y to enforce the boundary condition $\frac{\partial\phi}{\partial n} = 0$. So, we could use two different FD approximations for the normal derivative on the waveguide boundary:

$$\left.\frac{\partial\phi}{\partial n}\right|_X \simeq \frac{\phi_X - \phi_P}{\Delta u/2} \qquad \text{or} \qquad \left.\frac{\partial\phi}{\partial n}\right|_X \simeq \frac{\phi_Y - \phi_P}{\Delta u} \qquad (10)$$

The first one avoids an extrapolation outside the waveguide region, but has an error $\mathcal{O}(\Delta u/2)$, whereas the second one is more accurate, with

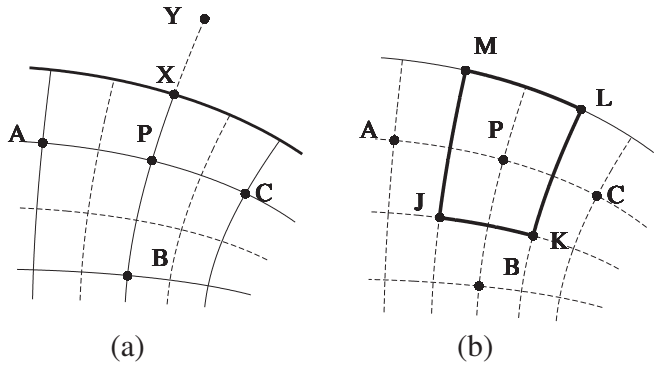

Figure 4. (a) Sampling points for ϕ_{TE} in the boundary region (TE grid); (b) Geometry pertinent to the boundary point P in the TE case, the curve Γ_F consists of the bold lines joining J-K-L-M.

an error $\mathcal{O}(\Delta u^2)$, but needs a ϕ value outside the waveguide. Since both approximations have a drawback, we prefer to use the approach based on (5) instead. The curve Γ_F has four sides, and joins points J-K-L-M in Figure 4(b), and

$$\int_{\Gamma_F} \frac{\partial \phi}{\partial n}\, dl = \left\{ \int_J^K + \int_K^L + \int_L^M + \int_M^J \right\} \frac{\partial \phi}{\partial n}\, dl \tag{11}$$

Now, on the segment LM the integrand is equal to zero because of (2), whereas on the others sides we have, using a finite approximation of the derivatives

$$\begin{aligned} &\text{on } JK \qquad \frac{\partial \phi}{\partial n} = \frac{\phi_B - \phi_P}{h_P \Delta u} \\ &\text{on } KL \qquad \frac{\partial \phi}{\partial n} = \frac{\phi_C - \phi_P}{h_P \Delta v} \\ &\text{on } MJ \qquad \frac{\partial \phi}{\partial n} = \frac{\phi_A - \phi_P}{h_P \Delta v} \end{aligned} \tag{12}$$

Putting (12) in (11), we find that (7) is replaced, for a point P as in Figure 4, by:

$$\frac{(\phi_C - \phi_P)}{h_P \Delta v} L_E + \frac{(\phi_A - \phi_P)}{h_P \Delta v} L_E + \frac{(\phi_B - \phi_P)}{h_P \Delta u} L_I = -k_t^2 \phi_P \; S_A \tag{13}$$

where $h_P = a\sqrt{\sinh^2 u_P + \sin^2 v_P}$ is the scale factor of the elliptic cylindrical coordinate, evaluated in P and $S_A = h_P^2 \Delta u \Delta v$ the area of the cell. $L_I = h_P \Delta v$ and $L_E = h_P \Delta u$ are the lengths of the sides of the cell. Equation (13) can be reordered as:

$$\frac{\phi_A}{h_P^2 \Delta v^2} + \frac{\phi_C}{h_P^2 \Delta v^2} + \frac{\phi_B}{h_P^2 \Delta u^2} - \frac{2\phi_P}{h_P^2} \left(\frac{1}{2\Delta u^2} + \frac{1}{\Delta v^2} \right) = -k_t^2 \phi_P \tag{14}$$

If we use the second of (10) to enforce the TE boundary condition (2), we will derive that this BC is equivalent to $\phi_Y = \phi_P$ (see Figure 4). Now, if we apply (8) to point P, including Y as point $(i+1, j)$, and let $\phi_Y = \phi_P$, we obtain the exact discretized Equation (14). Therefore, we can conclude that the TE boundary condition can be approximated, in FD terms, by $\phi_Y = \phi_P$. This has been considered, actually, in the literature up to now but, to the best of our knowledge, without a proof (except, perhaps, some error considerations like the ones we have made after (10)).

2.2.2. Singularity Points

For a point P lying on the segment joining the two foci (see Figure 5(a)), we have $u = 0$. Therefore, P is a singular point (more

precisely a *cusp*) of the framework, but the potential must be regular here. As a consequence, only (5) can be used for the approximation of (1). In this case, we select the curve Γ_F in (5) as the bold curve *J-K-L-M* in Figure 5(a). Since no framework singularities are present on Γ_F, a simple finite difference approximation of the integral gives:

$$\frac{(\phi_C-\phi_P)}{h_P\Delta v}L_E+\frac{(\phi_A-\phi_P)}{h_P\Delta v}\cdot L_E+\frac{(\phi_B-\phi_P)}{h_P\Delta u}L_I + \frac{(\phi_D-\phi_P)}{h_P\Delta u}L_I=-k_t^2\phi_p\ S_A \tag{15}$$

wherein $h_P = a\sin v_P$ is the scale factor of the elliptic cylindrical coordinate, evaluated in P (in this case, in P, $u = 0$). Equation (15) can be reordered as:

$$\frac{\phi_A+\phi_C}{h_P^2\Delta v^2}+\frac{\phi_B+\phi_D}{h_P^2\Delta u^2}-\frac{2\phi_P}{h_P^2}\left(\frac{1}{\Delta u^2}+\frac{1}{\Delta v^2}\right)=-k_t^2\phi_P \tag{16}$$

For the foci, the approach is the same. We apply (5) using, as curve Γ_F, the bold curve $K-L$ in Figure 5(b). The cell S_F is bounded by the ellipse at $u = \Delta u/2$, and by the branch of the hyperbola at $v = \Delta v/2$ (intersecting in K and L). If $\hat{S}$ is the area of the cell, we get from (5):

$$\frac{1}{\hat{S}}\left[(\phi_C-\phi_P)\cdot 2L_e+(\phi_A-\phi_P)\cdot 2L_i\right]=-k_t^2\phi_P \tag{17}$$

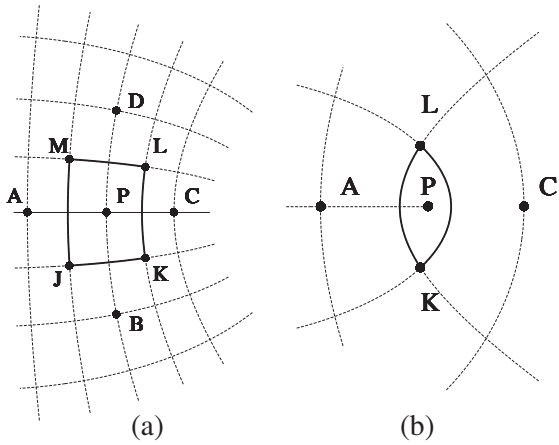

Figure 5. (a) Geometry relevant to a point P lying on the segment joining the two foci; (b) geometry relevant to a focus P of the framework.

wherein L_e and L_i are half the length of the arc of the ellipse and of the arc of the hyperbola, respectively. These can be computed from the scale factor $h(u, v)$ as:

$$\begin{aligned} L_e &= \int_0^{\frac{\Delta v}{2}} h\left(\frac{\Delta u}{2}, v\right) dv \cong \frac{\Delta v}{4}\left(h\left(\frac{\Delta u}{2}, 0\right) + h\left(\frac{\Delta u}{2}, \frac{\Delta v}{2}\right)\right) \\ L_i &= \int_0^{\frac{\Delta u}{2}} h\left(u, \frac{\Delta v}{2}\right) du \cong \frac{\Delta u}{4}\left(h\left(0, \frac{\Delta v}{2}\right) + h\left(\frac{\Delta u}{2}, \frac{\Delta v}{2}\right)\right) \end{aligned} \tag{18}$$

2.2.3. Use of a Single Grid for TE *and* TM *Modes*

TE modes are given by the eigenvalues and eigenvectors of $(8, 14, 16, 17)$, and TM ones by $(8, 9, 16, 17)$. Both matrices are sparse, so very effective routines can be used to compute them [31]. However, the resulting TE waveguide modes are known on a different set of sampling points than TM modes. Since those sets are not easily mapped one onto the other (compare Figure 2), this is a significant drawback. Therefore, we consider here also the use of a single grid, namely the TE one, for all modes, either TE or TM. This requires only to rephrase the FD approximation of the BC (2) of TM modes to be implemented on the TE grid (Figure 2(a)).

Let us consider a boundary point P in this grid, as in Figure 6. The point D does not belong to the discretization set, but we can enforce the BC $\phi_D = 0$ expressing the potential ϕ_D through a Taylor approximation:

$$\phi_D = \phi_P + \left.\frac{\partial \phi}{\partial u}\right|_P \frac{\Delta u}{2} + \frac{1}{2}\left.\frac{\partial^2 \phi}{\partial u^2}\right|_P \left(\frac{\Delta u}{2}\right)^2 = 0 \tag{19}$$

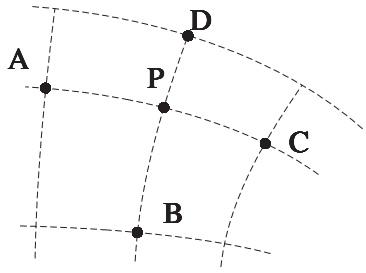

Figure 6. Geometry relevant to enforce TM boundary condition onto a TE grid (the point D does not belong to the discretization grid).

which, together with

$$\phi_B = \phi_P + \left.\frac{\partial\phi}{\partial u}\right|_P (-\Delta u) + \frac{1}{2}\left.\frac{\partial^2\phi}{\partial u^2}\right|_P (-\Delta u)^2 \tag{20}$$

gives:

$$\left.\frac{\partial^2\phi}{\partial u^2}\right|_P = \frac{4}{3\Delta u^2}\,(\phi_B - 3\phi_P) \tag{21}$$

The final expression is therefore:

$$\begin{aligned}\left[\frac{\partial^2\phi}{\partial u^2} + \frac{\partial^2\phi}{\partial v^2}\right]_P = {} & \frac{1}{\Delta v^2}\cdot\phi_A + \frac{1}{\Delta v^2}\cdot\phi_C \\ & + \frac{4}{3\cdot\Delta u^2}\cdot\phi_B - \left(\frac{4}{\Delta u^2} + \frac{2}{\Delta v^2}\right)\cdot\phi_P\end{aligned} \tag{22}$$

In this way, replacing (9) with (22) gives the TM modes computed in the TE grid shown in Figure 2(a).

3. NUMERICAL RESULTS

The curvilinear FDFD method described in the previous section has been extensively tested using data available in the open literature. We have selected the cut-off frequency data from [16], which span the whole eccentricity range. These data appear to be quite accurate but have been obtained by a method which is both heavy and with a reduced flexibility. A further comparison has been made with the standard FDFD results, obtained with a staircase approximation of the boundary.

The results presented in this section consider three values of the eccentricity e, the ones presented in [16], namely $e = 0.1$, $e = 0.5$, $e = 0.9$. All dimensions have been normalized to the minor semi-axis of the ellipse.

In Figure 7 we show the main validation test. We have compared the TE data obtained using the proposed FDFD approach with the data of [16] for the case $e = 0.5$.

Different discretization steps have been considered, both for Δu and for Δv, and the selected steps lead to 18000, 36000 and 72000 discretization points, respectively. The results for a standard FDFD approach, using a staircase approximation of the boundary have been included, too. The latter have been computed using 144000 and 581000 discretization points ($\Delta x = \Delta y = 0.01995$ or 0.00999), and therefore require a significantly larger computational cost. As a matter of fact, the computational cost depends only on the number of discretization points.

TM error data are completely equivalent.

From the results presented in Figure 7, it appears that the use of a curvilinear discretization grid allows to compute k_t, i.e., the mode cut-off frequency, with a relative error consistently lower than 0.1% for all modes using only 18000 points. On the other hand, the standard FDFD

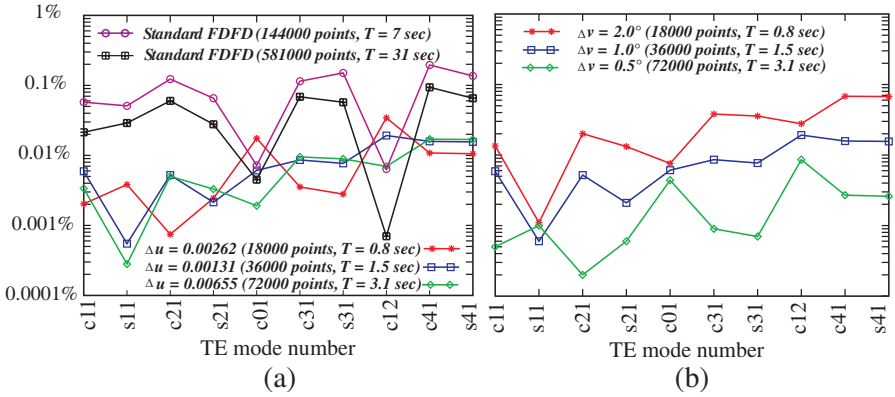

Figure 7. Relative error on k_t of the proposed FDFD approach for the first TE modes. (a) $\Delta v = 1°$; (b) $\Delta u = 0.0131$. For comparison, in (a), the relative error for the standard FDFD approach (staircase approximation of the boundary) is also shown.

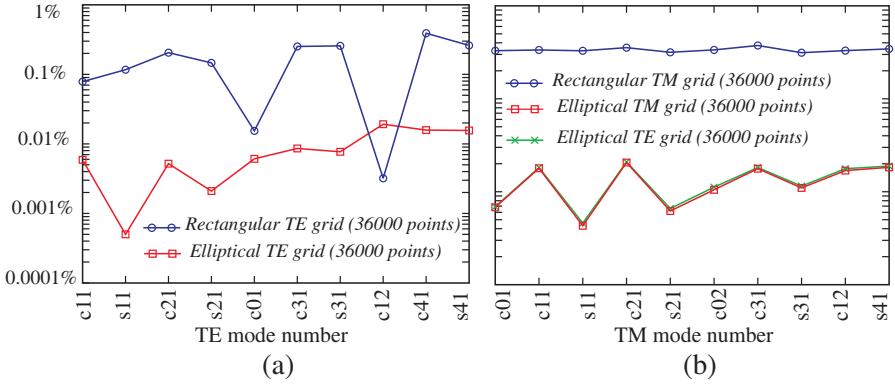

Figure 8. Relative errors on k_t at equal discretization points (36000). (a) First TE modes for the proposed FD approach (on the TE grid) and standard FD approach; (b) first TM modes for the proposed FD approach (both on the TM and TE grids) and standard FD approach. The discretization steps are $\Delta u = 0.0131$ and $\Delta v = 1°$ for the elliptical grid, $\Delta x = \Delta y = 0.0389$ for the rectangular grid.

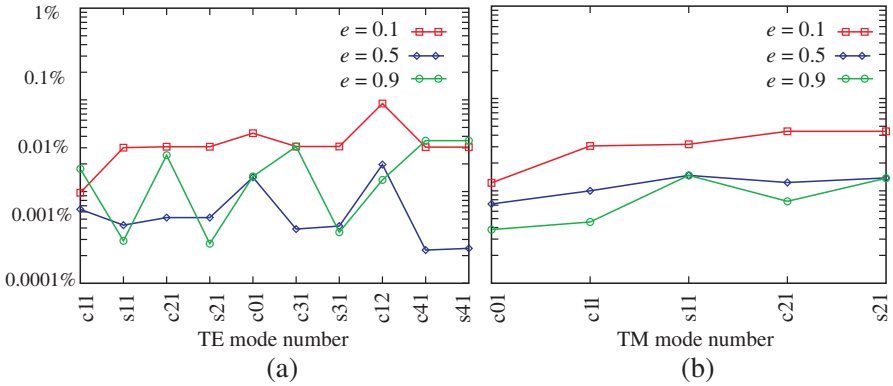

Figure 9. Relative error on k_t of the proposed FD approach for different eccentricities. (a) First TE modes of an elliptic guide (TE elliptical grid); (b) first TM modes of an elliptic guide (TE elliptical grid). $\Delta u = 0.0262$ and $\Delta v = 0.5°$, corresponding to 36000 points.

approach requires 581000 points to give a comparable accuracy (i.e., a relative error lower than 0.1% for all modes). Moreover, the relative error of the curvilinear approach is stable for different waveguide modes, whereas that of the standard FDFD is not. In Figure 7, the computational time T required to compute the eigenvalues (on a PC with two Intel Xeon E5504 CPUs@2.00 GHz, 48 GB RAM, OS: MS Windows 7 Professional) is also reported.

In Figure 8, we show a comparison between our approach and the standard FDFD (staircase approximation) with the same number of discretization points, and so the same computational complexity. We have considered both TE modes (Figure 8(a)) and TM modes (Figure 8(b)), the latter also on the TE grid (in order to test the case of a single grid both for TE and TM modes). From Figures 8(a) and 8(b), it is apparent that our approach allows an accuracy typically larger than about one order of magnitude respect to the standard FDFD. Moreover, this accuracy does not depend on the chosen grid, since use of either a tailored TM grid (Figure 2(b)), or an uncorrelated grid (Figure 2(a)) gives the same accuracy (see Figure 8(b)).

The proposed FD approach thus allows a significant accuracy, both on the eigenvalues (i.e., the cut-off frequency and propagation constant of those modes), and on the mode distribution.

Finally, we have tested the effect of the eccentricity on the accuracy of the solution. The results, reported in Figure 9(a) for TE modes, and in Figure 9(b) for the TM modes (on the TE grid), show that the accuracy usually increases with the eccentricity, but remains of the same order of magnitude.

4. CONCLUSION

A new approach to the FD computation of modes of an elliptic waveguide has been presented. The main idea is the use of a discretization grid tailored to the waveguide boundary. In this way, the curved boundary is exactly described, using only a fraction of the discretization points required by the standard rectangular grid (which is only approximate). The use of a single TE grid for all (TE and TM modes) has been assessed. This allows to implement numerical procedures requiring all modes, such as Mode Matching, in an easier way. The results presented show the effectiveness (accuracy vs. computational cost) of the approach described here.

REFERENCES

1. Conciauro, G., et al., "Waveguide modes via an integral equation leading to a linear matrix eigenvalue problem," *IEEE Trans. Microwave Theory Techniques*, Vol. 32, 1495–1504, 1984.
2. Accatino, L., et al., "Elliptical cavity resonators for dual-mode narrowband filters," *IEEE Trans. Microwave Theory Techniques*, Vol. 45, 2393–2401, 1997.
3. Wexler, A., "Solution of waveguide discontinuities by modal analysis," *IEEE Trans. Microwave Theory Techniques*, Vol. 15, 508–517, 1967.
4. Chan, K. L. and S. R. Judah, "Mode-matching analysis of a waveguide junction formed by a circular and a larger elliptic waveguide," *IEE Proc. Microw. Antennas Propag.*, Vol. 145, 123–127, 1998.
5. Collin, R. E., *Field Theory of Guided Waves*, 2nd Edition, Ch. 7, Wiley-IEEE Press, New York, 2001.
6. Mazzarella, G. and G. Montisci, "Accurate modeling of coupling junctions in dielectric covered waveguide slot arrays," *Progress In Electromagnetics Research M*, Vol. 17, 59–71, 2011.
7. Montisci, G., G. Mazzarella, and G. A. Casula, "Effective analysis of a waveguide longitudinal slot with cavity," *IEEE Trans. Antennas Propag.*, Vol. 60, 3104–3110, 2012.
8. Mazzarella, G. and G. Montisci, "Wideband equivalent circuit of a centered-inclined waveguide slot coupler," *Journal of Electromagnetic Waves and Applications*, Vol. 14, No. 1, 133–151, 2000.
9. Casula, G. A., G. Mazzarella, and G. Montisci, "Effective analysis

of a microstrip slot coupler," *Journal of Electromagnetic Waves and Applications*, Vol. 18, No. 9, 1203–1217, 2004.

10. Mazzarella, G. and G. Montisci, "A rigorous analysis of dielectric-covered narrow longitudinal shunt slots with finite wall thickness," *Electromagnetics*, Vol. 19, 407–418, 1999.
11. Mazzarella, G. and G. Montisci, "Accurate characterization of the interaction between coupling slots and waveguide bends in waveguide slot arrays," *IEEE Trans. Microwave Theory Techniques*, Vol. 48, 1154–1157, 2000.
12. Casula, G. A., G. Mazzarella, and G. Montisci, "Effect of the feeding t-junctions in the performance of planar waveguide slot arrays," *IEEE Antennas and Wireless Propag. Letters*, Vol. 11, 953–956, 2012.
13. Chu, L. J., "Electromagnetic waves in elliptic hollow pipes of metal," *J. Appl. Phys.*, Vol. 9, 583–591, 1938.
14. Marcuvitz, N., *Waveguide Handbook*, Peregrinius, London, 1986.
15. Kretzschmar, J. G., "Wave propagation in hollow conducting elliptical waveguides," *IEEE Trans. Microwave Theory Techniques*, Vol. 18, 547–554, 1970.
16. Zhang, S. and Y. Chen, "Eigenmodes sequence for an elliptical waveguides with arbitrary ellipticity," *IEEE Trans. Microwave Theory Techniques*, Vol. 43, 227–230, 1995.
17. Shu, C., "Analysis of elliptical waveguides by differential quadrature method," *IEEE Trans. Microwave Theory Techniques*, Vol. 48, 319–322, 2000
18. Weiland, T., "Three dimensional resonator mode computation by finite difference method," *IEEE Trans. Magn.*, Vol. 21, 2340–2343, 1985.
19. Fanti A., G. Mazzarella, and G. Montisci, "Curvilinear vector finite difference approach to the computation of waveguide modes," *Advanced Electromagnetics*, Vol. 1, 29–37, 2012.
20. Zhao, Y. J., K. L. Wu, and K. K. M. Cheng, "A compact 2-D full-wave finite-difference frequency-domain method for general guided wave structures," *IEEE Trans. Microwave Theory Techniques*, Vol. 50, 1844–848, 2002.
21. Hwang, J. N., "A compact 2-D FDFD method for modeling microstrip structures with nonuniform grids and perfectly matched layer," *IEEE Trans. Microwave Theory Techniques*, Vol. 53, 653–59, 2005.
22. Kuzu, L., V. Demir, A. Z. Elsherbeni, and E. Arvas, "Electromagnetic scattering from arbitrarily shaped chiral objects

using the finite difference frequency domain method," *Progress In Electromagnetics Research*, Vol. 67, 1–24, 2007.

23. Podwalski, J., P. Kowalczyk, and M. Mrozowski, "Efficient multiscale finite difference frequency domain analysis using multiple macromodels with compressed boundaries," *Progress In Electromagnetics Research*, Vol. 126, 463–479, 2012.
24. Rumpf, R. C., "Simple implementation of arbitrarily shaped total-field/scattered-field regions in finite-difference frequency-domain," *Progress In Electromagnetics Research B*, Vol. 36, 221–248, 2012.
25. Lovranos, C. S. and G. A. Kyriacou, "Eigenvalue analysis of curved waveguides employing an orthogonal curvilinear frequency-domain finite-difference method," *IEEE Trans. Microwave Theory Techniques*, Vol. 57, 594–611, 2009.
26. Taflove, A., *Advances in Computational Electrodynamics — The FDTD Method*, Artech House, London, 1995.
27. Xiao, S., R. Vahldieck, and H. Jin, "Full-wave analysis of guided wave structures using a novel 2-D FDTD," *IEEE Microwave Guided Wave Lett.*, Vol. 2, 165–67, 1992.
28. Choi, D. H. and W. J. R. Hoefer, "The finite-difference-time-domain method and its applications to eigenvalue problems," *IEEE Trans. Microwave Theory Techniques*, Vol. 34, 1464–470, 1986.
29. Fanti, A. and G. Mazzarella, "Finite differences single grid evaluation of TE and TM modes in metallic waveguides," *Loughborough Antennas Propag. Conf.*, 517–520, Loughborough, UK, 2010.
30. Itoh, T., *Numerical Techniques for Microwave and Millimeter-wave Passive Structures*, Sect. 1.1, Wiley, New York, 1989.
31. Golub, G. H. and C. F. Van Loan, *The Matrix Computations*, 3rd Edition, The Johns Hopkins University Press, Baltimore MD, 1996.